JOURNAL OF SCIENCE TECHNOLOGY AND EDUCATION 8(3), SEPTEMBER, 2020
ISSN: 2277-0011; Journal homepage: www.atbuftejoste.com

Modelling and Optimisation of High Pressure Water Scrubbing of Biogas for CO_2 removal using Response Surface Methodology and Artificial Neural Networks

[1]Muhammad, I. J., [2]Amenaghawon, N. A. and [3]Ajieh, M. U.
[1]Department of Gas Development,
Nigerian Petroleum Development Company, Benin City, Edo State, Nigeria
[2]Department of Chemical Engineering,
Faculty of Engineering, University of Benin, Benin City, Edo State, Nigeria
[3]Department of Chemical Engineering,
Delta State University, Oleh Campus, Delta State, Nigeria

ABSTRACT

Biogas produced from anaerobic digestion of organic wastes consists of mainly methane (CH_4) and undesirable gases like carbon dioxide (CO_2), hydrogen sulphide (H_2S) and other trace gases. This study focused on the modelling and optimisation of biogas upgrading using high pressure water scrubbing (HPWS). The biogas upgrading process was simulated using Aspen HYSYS while the experiments were designed using Design Expert software. Response surface methodology (RSM) and artificial neural network (ANN) was adopted to model and optimise the process. The four factors considered were absorber pressure, biogas flowrate, and water flow rate and absorber temperature. RSM analysis yielded a quadratic model for predicting the chosen responses (CH_4 recovered and CO_2 captured) as a function of the four independent variables. For ANN, a multilayer full feed forward neural network trained with the Levenberg-Marquardt algorithm was found suitable for modelling the upgrading process. Both the RSM and ANN models described the upgrading process (methane recovery) with high accuracy as indicated by their high R^2 (0.9826 and 0.9999), low RMSE (1.3937 and 0.1200) and low AAD (0.0172 and 0.0006) values respectively. Optimisation results showed that up to 93% CH_4 recovery and 87% CO_2 capture was achieved using HPWS and this was obtained at a condition of absorber pressure (18 bar), biogas flowrate (7 m^3/h), water flow rate (148 m^3/h) and absorber temperature (11 ^oC). When compared, the ANN model performed better in predicting the responses than RSM.

ARTICLE INFO

Article History
Received: March, 2020
Received in revised form: May, 2020
Accepted: July, 2020
Published online: September, 2020

KEYWORDS

Biogas, Carbon dioxide, ANOVA, HPWS, RSM, Optimisation

INTRODUCTION

Biogas is produced by anaerobic decomposition of organic substances, a process that is catalysed by a consortium of microorganisms (Zhang et al., 2017). Biogas consists mainly of methane (CH_4), carbon dioxide (CO_2), hydrogen sulphide (H_2S) and other gases such as water vapour, ammonia and nitrogen (Ajieh *et al*., 2016; Malinauskaite et al., 2017).

In its purified form, biogas can be used as a substitute for natural gas and be compressed and injected into the national gas pipeline network, thus becoming a valuable renewable energy source (Maria, 2008). However, the presence of undesirable components like

Corresponding author: Ajieh, M. U. ✉ *mike.ajieh@gmail.com* ✉ *Department of Chemical Engineering, Delta State University, Oleh Campus, Delta State, Nigeria.* *© 2020. Faculty of Tech. Education, ATBU Bauchi. All rights reserved*

carbon dioxide, water vapour, ammonia, hydrogen sulphide etc in biogas reduces its heating value and could potentially cause corrosion problems in the gas pipelines. The presence of these impurities in biogas can also potentially increase compression and transportation costs (Abdeen et al., 2016). This thus limits the application of biogas for power generation (Awe et al., 2017).

Thus, it is necessary to remove the impurities in biogas to improve its calorific value and enhance its fuel properties through an upgrading process (Sun et al., 2015). Currently, biogas upgrading strategies developed for industrial-scale operation include adsorption, chemical absorption, membrane separation and cryogenic processes (Khan et al., 2017). These methods are characterised by certain significant demerits such as high cost of deployment and environmental unfriendliness (IEA 2000).

However, high pressure water scrubbing has emerged as the most common strategy for biogas upgrading. This process is built on the basis of the fact that the impurity gases are more soluble in water than methane. For this process, water is used as a scrubbing solvent and the process takes place in a packed column in which water and biogas are contacted counter-currently (Petersson and Wellinger, 2009). Methane purity of as much as 80-99% have been recorded for biogas upgraded with high pressure water scrubbing pointing to the efficiency of the process (Cozma et al., 2015). The process is also accompanied by very little methane loss (3-5%) originating from the dissolution of methane in water.

The performance of the HPWS upgrading process has been reported to be dependent on a number of process variables such as pressure, temperature, composition, gas and liquid flowrate (Cozma et al., 2015; Kapoor et al., 2017). The efficiency of the process can be improved by optimizing these variables to give maximum methane recovery and carbon dioxide removal. This can be achieved by deploying techniques like design of experiment for response surface methodology (RSM) which is an empirical statistical tool for modelling and optimising multivariable processes (Amenaghawon et al., 2015). Recently, machine learning tools like artificial neural networks (ANN) have been deployed for modelling chemical engineering processes as a result of some of the limitations of RSM (Bas¸ and Boyaci, 2007). ANN is particularly useful when it is not possible to deploy conventional empirical models or when such models are inadequate in describing real life systems (Velu et al., 2016).

Thus, the aim of this study was to model and optimise high pressure water scrubbing of biogas for improved methane composition using RSM and ANN.

METHODOLOGY

Description of Biogas Upgrading Process

High pressure water scrubbing was adopted to upgrade the biogas produced in order to improve its fuel properties. The primary basis for achieving this was to remove the major impurities such as carbon dioxide and hydrogen sulphide. The description of the procedures for the production and characterisation of the biogas has been previously reported (Ajieh et al., 2018).

A simple process flow diagram of the water scrubbing process is shown in Figure 1. The basis of separation of the impurities is the difference in their solubility in water. When compared to CH_4, CO_2 and H_2S are relatively more soluble in water, hence they are preferentially separated from raw biogas. A high column pressure is usually used for this process to facilitate the separation process by increasing the driving force of solubility

Corresponding author: Ajieh, M. U. ✉ mike.ajieh@gmail.com ✉ Department of Chemical Engineering, Delta State University, Oleh Campus, Delta State, Nigeria. *© 2020. Faculty of Tech. Education, ATBU Bauchi. All rights reserved*

JOURNAL OF SCIENCE TECHNOLOGY AND EDUCATION 8(3), SEPTEMBER, 2020
ISSN: 2277-0011; Journal homepage: www.atbuftejoste.com

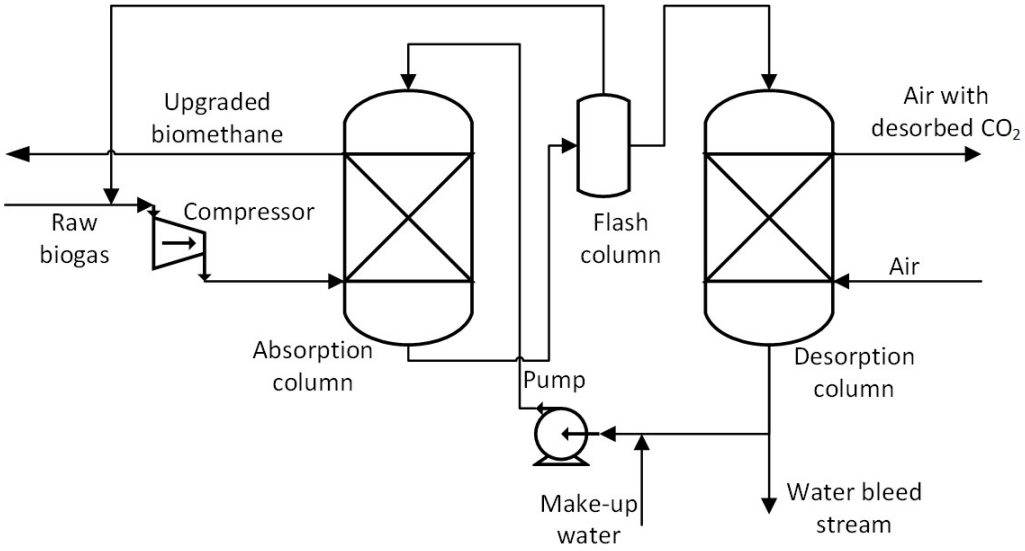

Figure 1: Process flow for water scrubbing process

Design of Experiment

In this study, a four variable Box-Behnken design (BBD) was used to plan the biogas upgrading experiments. The BBD was chosen for this purpose because it a very useful experimental design method and it is very suitable for fitting quadratic response surfaces, which are mostly encountered in many nonlinear processes in chemical engineering (Foroughi et al., 2018). For this work, the Design Expert® software version 7.0.0, (Stat-ease, Inc. Minneapolis, USA) was used to design the experiments and analyse the data obtained. The factors considered for optimisation are shown in Table 1. The range of these factors was selected based on previous studies and the operating conditions of real life biogas upgrading plants. The values of the factors were calculated using Equation 1.

$$x_i = \frac{X_i - X_o}{\Delta X_i} \qquad (1)$$

X_i and x_i are the actual and coded values of the factors respectively while X_o is the actual value of the factors at the centre point, and ΔX_i is the step change in the value of the actual values of the factors.

Equation 2 is a quadratic response model which was used to fit the experimental data and this was achieved by using multiple regression analysis to estimate the values of the coefficients of the model. The second order model was chosen because it is the most widely used model for response surface methodology is the most commonly used model for modelling real life processes (Asfaram et al., 2016). Analysis of variance (ANOVA) was then used to assess the quality and significance of the model.

$$Y = b_o + \sum_{i=1}^{N} b_i X_i + \sum_{i,j=1}^{N} b_{ij} X_i X_j + \sum_{i=1}^{N} b_{ii} X_i^2 + \sum_{i=1}^{N} e_i \qquad (2)$$

The optimisation of process variables and experimental conditions using RSM was through numerical optimisation methods (Myers et al., 2009).

Corresponding author: Ajieh, M. U. ✉ mike.ajieh@gmail.com ✉ Department of Chemical Engineering, Delta State University, Oleh Campus, Delta State, Nigeria. *© 2020. Faculty of Tech. Education, ATBU Bauchi. All rights reserved*

JOURNAL OF SCIENCE TECHNOLOGY AND EDUCATION 8(3), SEPTEMBER, 2020
ISSN: 2277-0011; Journal homepage: www.atbuftejoste.com

Table 1: Coded and actual level of factors for HPWS

Factors	Unit	Symbols	Actual and Coded Levels		
			-1	0	1
Absorber pressure	Bar	X_1	5	12.5	20
Biogas flowrate	m^3/h	X_2	7	9.5	12
Water flow rate	m^3/h	X_3	50	125	200
Absorber temperature	°C	X_4	5	22.5	40

Artificial Neural Network Modeling

For this study, artificial neural networks used to model the responses representing the biogas upgrading process (CH_4 recovered and CO_2 captured). To achieve this, a commercially available ANN Software, NeuralPower, version 2.5 (C.P.C-X Software USA) was used. In order to choose the most appropriate network architecture, two options were evaluated and these are multilayer full feed forward (MFFF) and a multilayer normal feed forward (MNFF) neural networks. A number of training algorithms were also evaluated to train the networks. The two networks evaluated were trained using algorithms such as incremental back propagation (IBP), quick propagation (QP), generic algorithm (GA), batch back propagation (BBP), and Levenberg- Marquardt (LM) algorithm. The most suitable transfer function for the hidden and output layer was chosen amongst the sigmoid, hyperbolic tangent, Gaussian, linear and threshold linear. The optimum number of neurons needed for the hidden layer of the network was determined following an iterative process. For this process, 70% of the experimental data was used to train the networks, 15% was used for validation while the remaining 15% was used for testing the network. The selection of the best network architecture, training algorithm, best transfer function and optimum number of neurons was done on the basis of the root mean square error (RMSE) and coefficient of determination (R^2). The best alternative was chosen to be the one with the highest R^2 value and smallest RMSE value (Betiku et al., 2014).

$$R^2 = 1 - \frac{\sum_{i=1}^{n}(x_{a,i}-x_{p,i})^2}{\sum_{i=1}^{n}(x_{p,i}-x_{a,ave})^2} \quad (3)$$

$$RMSE = \sqrt{\frac{1}{n}\sum_{i=1}^{n}(x_{p,i}-x_{a,i})^2} \quad (4)$$

$$AAD = \frac{1}{n}\left(\sum_{i=1}^{n}\left(\frac{|(x_{a,i}-x_{p,i})|}{x_{a,i}}\right)\right)\times 100 \quad (5)$$

Where n is the number of experimental data, $x_{p,i}$ is the predicted

RSM and ANN Data Verification

The capacity of RSM and ANN to predict the responses was evaluated by comparing the results predicted by the RSM and ANN models with those of the actual experiments. The level of fit between the RSM and the ANN was assessed by using the coefficient of determination (R^2 value), absolute average deviation (AAD) and root mean square error (RMSE), as defined in Equations 3 to 5 (Amenaghawon and Amagbewan, 2017). It is desirable that the R^2 value be as close to unity as possible while the RMSE and AAD should be as small as possible (Yi et al., 2009).

Corresponding author: Ajieh, M. U. ✉ mike.ajieh@gmail.com ✉ Department of Chemical Engineering, Delta State University, Oleh Campus, Delta State, Nigeria. *© 2020. Faculty of Tech. Education, ATBU Bauchi. All rights reserved*

value, $x_{a,i}$ is the experimental values, $x_{a,ave}$ is the average experimental values, and $x_{p,ave}$ is the average predicted values.

HYSYS Simulation of the HPWS Process

The Aspen HYSYS software version 2006 was used to carry out all the simulation reported in this work. For this study, the components added for the water scrubbing process were methane, (main component in raw biogas), carbon dioxide, hydrogen sulphide and water. The selection of the components was on the basis of the composition of the actual biogas produced as reported in Ajieh et al. (2018). After creating the Component List, it was then associated with a Fluid Package. It is necessary to select the appropriate Fluid Package because the Fluid Package contains the thermodynamic models that are used by the Aspen HYSYS software to carry out vapour liquid equilibrium calculations (AspenTech 2017).

For the base case simulation, the raw biogas was compressed (in Comp. 1) to increase its pressure from 1 bar to about 2 bar. The composition of the raw biogas feed was determined through chromatographic analysis of the biogas produced from the anaerobic digestion of the organic waste feedstock as reported in Ajieh et al. (2018). After compressing the raw biogas to 2 bar, it was then cooled and further compressed and cooled in order to take it to the operating pressure of the absorber. The compressed raw biogas was fed to the absorption column (Absorber) from the bottom and it was made to contact the scrubbing water in a counter current manner (Figures 2 and 4). During this process, the water absorbs the CO_2 in the raw biogas and the upgraded biogas that is essentially methane (biomethane) is collected from the top of the absorption column. The water containing the absorbed impurities was sent to a flash drum (Flash separator) where the pressure was suddenly reduced to effect flash vapourisation. The gas stream from the flash separator was combined with the raw biogas at the start of the process using the mixer. The liquid stream from the flash separator which is mainly rich in CO_2 was then fed to the desorption column (stripper) and the absorbed CO_2 was removed using counter current flow of air at atmospheric pressure (Figures 3 and 4). The regenerated water was then recirculated back to the absorber. For the simulation process, some operating variables of the absorber were varied to determine the effect on methane recovery and CO_2 capture and this was done using the experimental design.

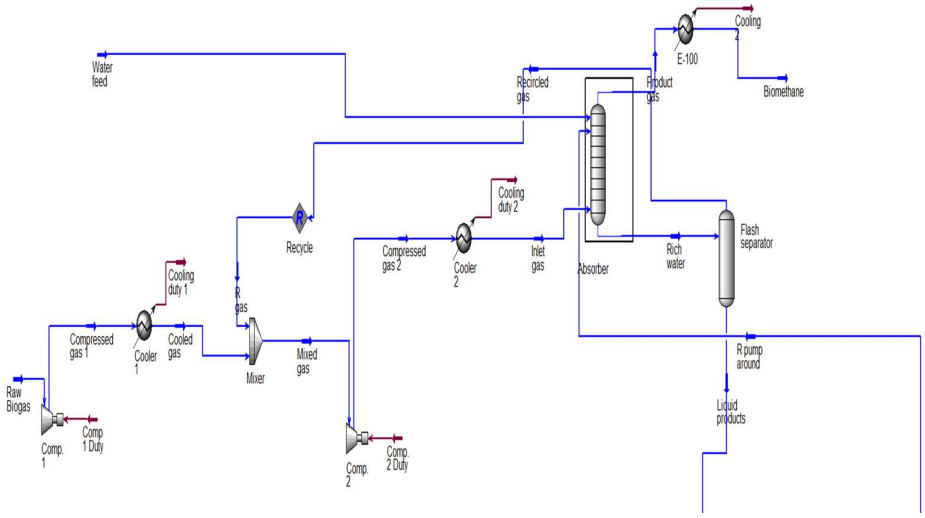

Figure 2: HYSYS process flow diagram for HPWS (absorber portion)

Corresponding author: Ajieh, M. U. ✉ mike.ajieh@gmail.com ✉ Department of Chemical Engineering, Delta State University, Oleh Campus, Delta State, Nigeria. *© 2020. Faculty of Tech. Education, ATBU Bauchi. All rights reserved*

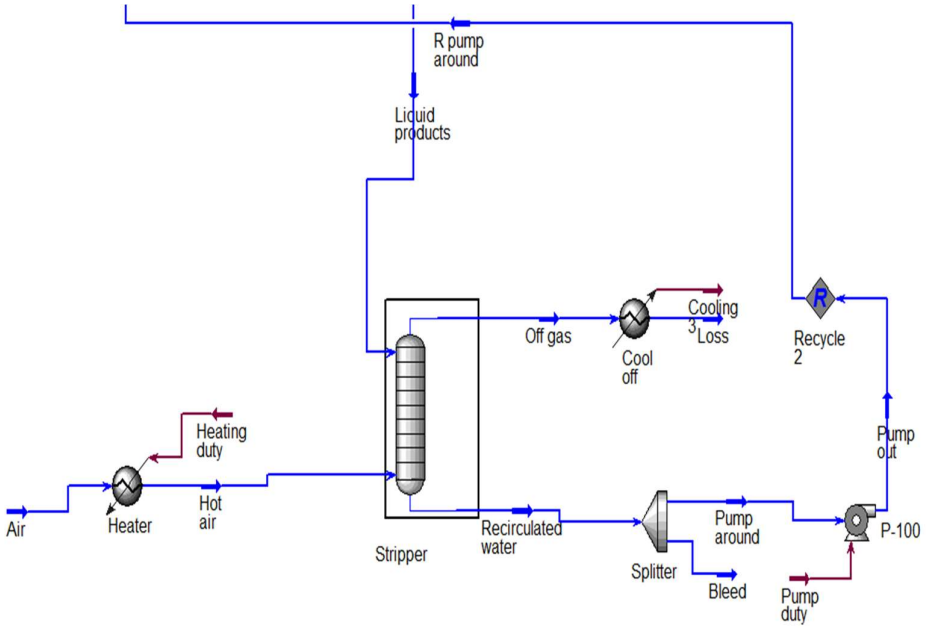

Figure 3: HYSYS process flow diagram for HPWS (stripper portion)

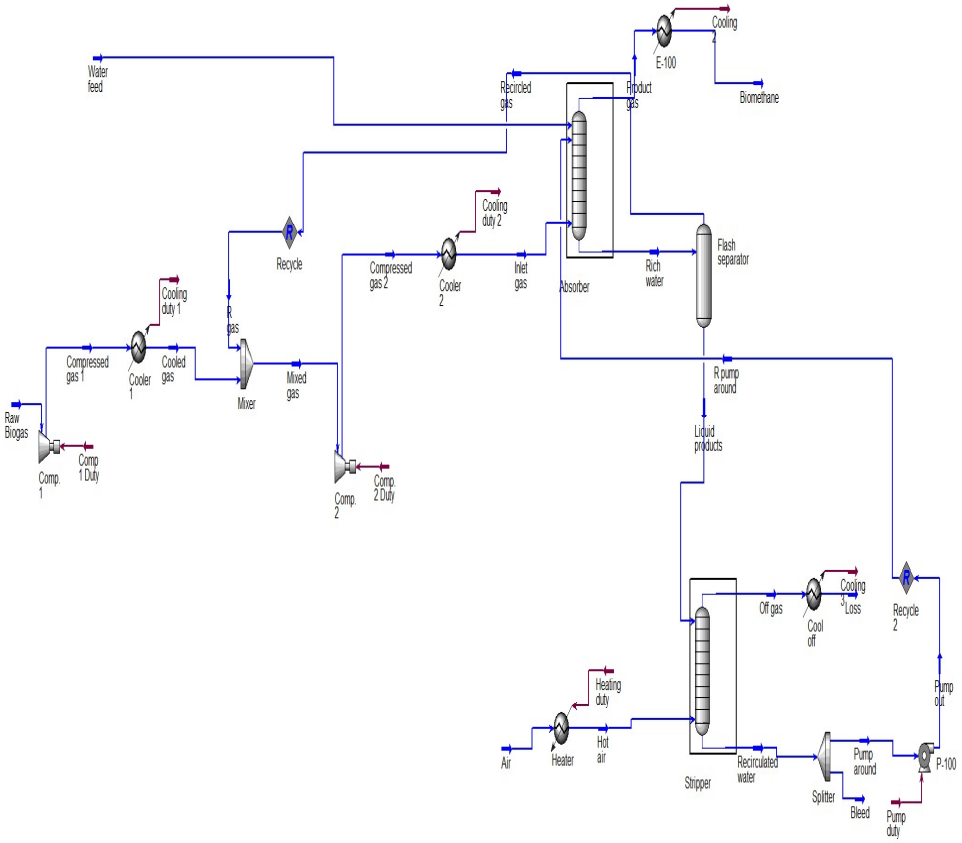

Figure 4: HYSYS process flow diagram for HPWS (full process flow diagram)

Corresponding author: Ajieh, M. U. ✉ *mike.ajieh@gmail.com* ✉ *Department of Chemical Engineering, Delta State University, Oleh Campus, Delta State, Nigeria.* *© 2020. Faculty of Tech. Education, ATBU Bauchi. All rights reserved*

Validation of HYSYS Thermodynamic Model

For this work, different thermodynamic models were evaluated to determine their suitability for the intended purpose. This was done because if the wrong thermodynamic model is chosen, it could lead to incorrect simulation results. The accuracy of the simulation results is tied to the selection of the appropriate thermodynamic model (Cozma et al., 2013). The models investigated were NRTL-Ideal (Non-Random-Two-Liquid with ideal gas and Henry's law), NRTL-RK (Non-Random-Two-Liquid/Redlich-Kwong equation of state with Henry's law), UNIQUAC-RK (Universal Quasi Chemical/Redlich-Kwong equation of state with Henry's law) and Wilson. These different models were validated using experimental data reported in the literature (Chapoy et al., 2004; Valtz et al., 2004). The thermodynamic model deemed to be most appropriate for the intended purpose was the one that showed the best fit with the experimental data. The most appropriate thermodynamic model was thus chosen to run all the simulations reported in this work.

RESULTS AND DISCUSSION

Validation of HYSYS Model

The applicability of the thermodynamic models in the HYSYS software was evaluated by comparing the model results with the available experimental literature data for CO_2 and CH_4 solubility in solution (Chapoy et al., 2004; Valtz et al., 2004). The results are shown in Figures 5 and 6. Figures 5 and 6 for CO_2 and CH_4 respectively show the comparison of the experimental data with the HYSYS models (NRTL-Ideal, NRTL-RK, UNIQUAC-RK, and Wilson). After comparing the results obtained for all four thermodynamic models, it was found that the NRTL-Ideal (Non-Random-Two-Liquid with ideal gas and Henry's law) model best fitted the experimental data and was thus used for the simulations done in the remainder of this work.

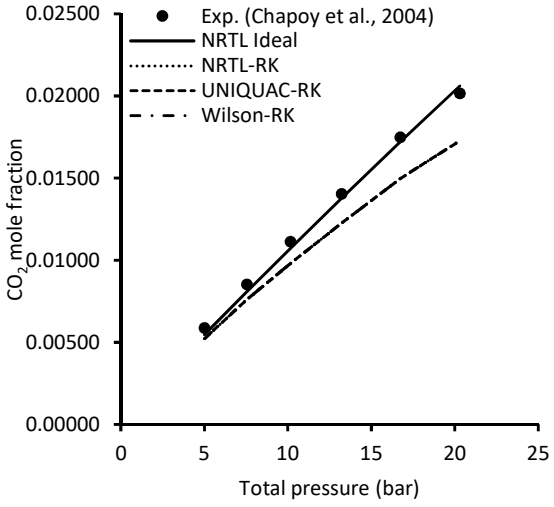

(a)

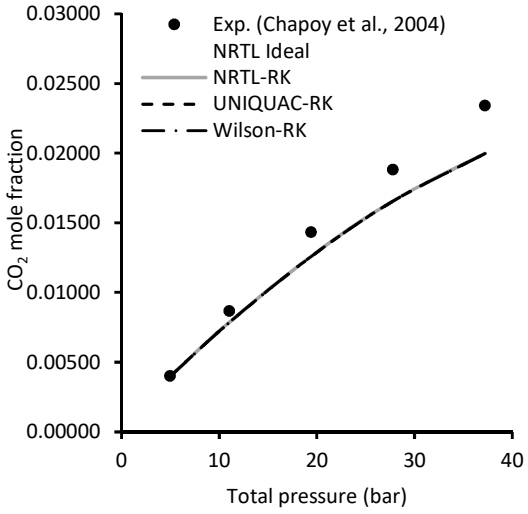

(b)

Corresponding author: Ajieh, M. U. ✉ *mike.ajieh@gmail.com* ✉ *Department of Chemical Engineering, Delta State University, Oleh Campus, Delta State, Nigeria.* *© 2020. Faculty of Tech. Education, ATBU Bauchi. All rights reserved*

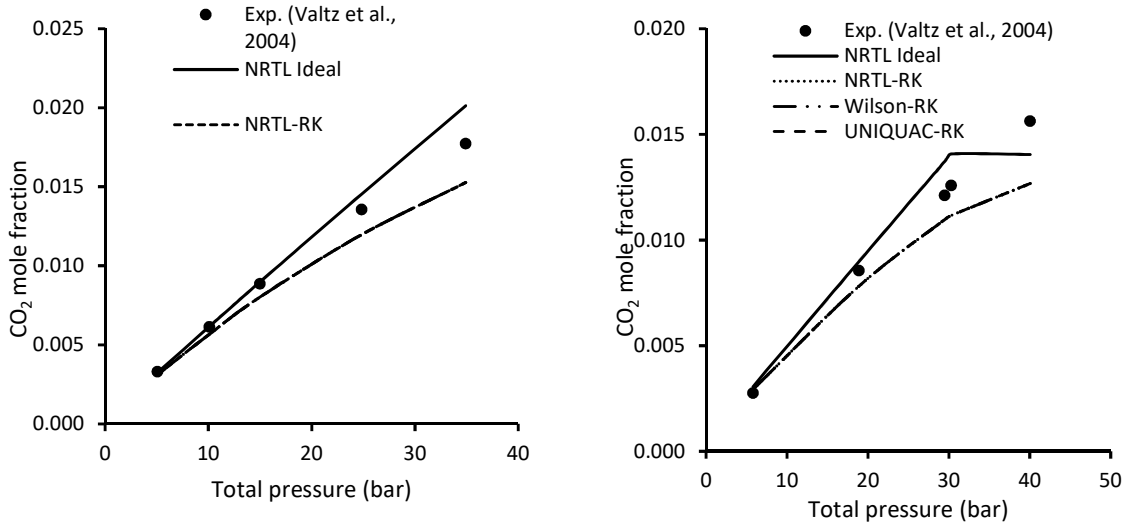

Figure 5: Comparison of model and experimental results of CO_2 solubility at (a) 5 °C (b) 15 °C (c) 25 °C (d) 35 °C

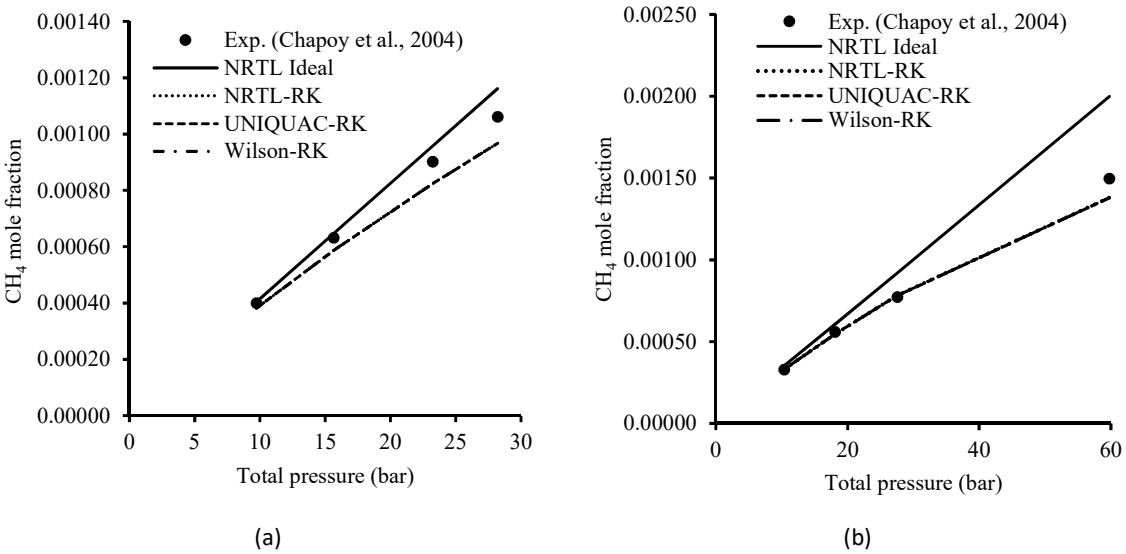

Corresponding author: Ajieh, M. U. ✉ *mike.ajieh@gmail.com* ✉ *Department of Chemical Engineering, Delta State University, Oleh Campus, Delta State, Nigeria.* *© 2020. Faculty of Tech. Education, ATBU Bauchi. All rights reserved*

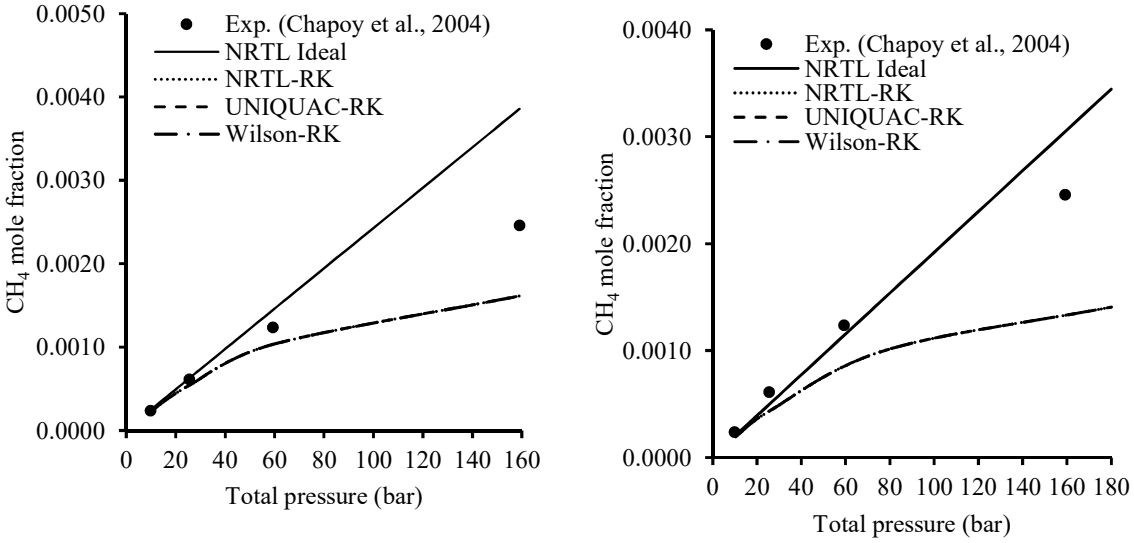

(c) (d)

Figure 6: Comparison of model and experiment results for CH_4 solubility at (a) 2 °C (b) 10 °C (c) 25 °C (d) 40 °C

Statistical Analysis of Models

The quadratic model was fitted to the data generated from the HYSYS simulations in order to estimate the model parameters. A total of 29 experimental runs were obtained by the Box-Behnken design for this purpose. Multiple regression analysis was used for the fitting process and the model parameters were estimated to obtain the final model equations in terms of actual experimental factors. The model equations for the two responses are shown in Equations 6 and 7. The equations represent CH_4 recovered and CO_2 captured as a function of absorber pressure (X_1), gas flow rate (X_2), liquid flowrate (X_3) and absorber temperature (X_4). These equations were used to predict their corresponding responses and the results are shown in Table 2. Comparison of the experimental values (HYSYS simulation) of the response and those predicted by the statistical models showed that there was an acceptable level of fit between the two as seen in the fact that both set of values were very close.

$$CH_4\ recovered = 63.45 + 3.56X_1 - 5.30X_2 + 0.34X_3 - 0.16X_4 + 0.034X_1X_2 - 0.016X_1X_3 - 0.011X_2X_3 + 0.0012X_2X_4 + 0.0018X_3X_4 - 0.057X_1^2 + 0.16X_2^2 - 0.00080X_3^2 + 0.0029X_4^2 \quad (6)$$

$$CO_2\ captured = 63.45 + 3.56X_1 - 5.30X_2 + 0.35X_3 - 0.17X_4 + 0.034X_1X_2 - 0.016X_1X_3 - 0.0000092X_1X_4 + 0.011X_2X_3 + 0.0012X_2X_4 + 0.00018X_3X_4 - 0.057X_1^2 + 0.16X_2^2 - 0.00080X_3^2 + 0.0029X_4^2 \quad (7)$$

Corresponding author: Ajieh, M. U. ✉ mike.ajieh@gmail.com ✉ Department of Chemical Engineering, Delta State University, Oleh Campus, Delta State, Nigeria. *© 2020. Faculty of Tech. Education, ATBU Bauchi. All rights reserved*

JOURNAL OF SCIENCE TECHNOLOGY AND EDUCATION 8(3), SEPTEMBER, 2020
ISSN: 2277-0011; Journal homepage: www.atbuftejoste.com

Table 2: Experimental and RSM predicted results

Run	Factors								Responses			
	Coded values				Actual values				CH_4 recovered (%)		CO_2 captured (%)	
	X_1	X_2	X_3	X_4	X_1	X_2	X_3	X_4	Exp.	RSM	Exp.	RSM
1	0	0	-1	-1	12.5	9.5	50	5.0	73.7	73.6	81.7	77.6
2	0	1	0	-1	12.5	12.0	125	5.0	77.5	78.8	85.4	86.7
3	1	-1	0	0	20.0	7.0	125	22.5	88.9	91.0	85.7	87.7
4	-1	0	1	0	5.0	9.5	200	22.5	64.7	64.6	84.9	87.7
5	-1	-1	0	0	5.0	7.0	125	22.5	65.2	67.5	85.4	81.2
6	0	-1	1	0	12.5	7.0	200	22.5	89.4	88.7	85.7	85.9
7	0	0	0	0	12.5	9.5	125	22.5	81.7	81.2	85.9	85.7
8	0	0	-1	1	12.5	9.5	50	40.0	73.4	74.4	80.8	77.0
9	1	0	0	-1	20.0	9.5	125	5.0	85.1	85.7	85.7	87.3
10	0	1	1	0	12.5	12.0	200	22.5	80.7	80.0	85.7	88.2
11	0	0	1	1	12.5	9.5	200	40.0	82.9	84.0	85.7	87.1
12	1	1	0	0	20.0	12.0	125	22.5	85.1	83.7	85.7	87.1
13	-1	1	0	0	5.0	12.0	125	22.5	64.0	62.8	82.8	78.0
14	0	0	0	0	12.5	9.5	125	22.5	81.1	81.2	85.7	85.7
15	0	0	0	0	12.5	9.5	125	22.5	81.1	81.2	85.7	85.7
16	1	0	-1	0	20.0	9.5	50	22.5	78.4	77.2	84.5	85.8
17	1	0	1	0	20.0	9.5	200	22.5	89.8	90.3	85.7	77.9
18	0	1	0	1	12.5	12.0	125	40.0	79.3	80.3	85.6	86.6
19	1	0	0	1	20.0	9.5	125	40.0	88.3	87.8	85.7	87.2
20	0	1	-1	0	12.5	12.0	50	22.5	71.9	73.0	75.8	74.3
21	-1	0	0	1	5.0	9.5	125	40.0	64.2	64.0	82.3	79.5
22	-1	0	0	-1	5.0	9.5	125	5.0	64.2	65.0	82.4	79.6
23	0	0	0	0	12.5	9.5	125	22.5	81.1	81.2	85.7	85.7
24	0	-1	-1	0	12.5	7.0	50	22.5	75.3	76.3	84.3	80.5
25	0	0	1	-1	12.5	9.5	200	5.0	83.7	83.5	85.7	86.7
26	0	0	0	0	12.5	9.5	125	22.5	81.1	81.2	85.7	85.7
27	0	-1	0	1	12.5	7.0	125	40.0	87.9	85.4	85.7	88.5
28	-1	0	-1	0	5.0	9.5	50	22.5	60.2	58.4	48.8	60.6
29	0	-1	0	-1	12.5	7.0	125	5.0	87.9	85.7	85.7	88.7

Analysis of Variance of Models

Analysis of variance (ANOVA) was carried out to assess the statistical significance and fit of the models representing the responses and the results are shown in Tables 3 and 4. Tables 3 and 4 show the ANOVA results for the models representing CH_4 recovered and CO_2 captured for the high-pressure water scrubbing process. For

Corresponding author: Ajieh, M. U. ✉ mike.ajieh@gmail.com ✉ Department of Chemical Engineering, Delta State University, Oleh Campus, Delta State, Nigeria. *© 2020. Faculty of Tech. Education, ATBU Bauchi. All rights reserved*

these results, model terms having p values less than 0.05 are significant. The implication of the statistical significance of a model is that changes in the values of the actual physical factor represented by that model term could potentially significantly affect the response under consideration. Conversely, model terms with p value greater than 0.05 are considered not to be significant and this also means that changes in the values of the actual physical factor represented by that model term does not significantly affect the response under consideration (Asfaram et al., 2016). The model terms representing absorber pressure (X_1), biogas flowrate (X_2), water flowrate (X_3) were significant in predicting both CH4 recovered and CO_2 captured as shown in Tables 3 and 4. Considering the results presented in Tables 3 and 4, it was observed that the "model p value" was in most cases < 0.0001. This indicates that the statistical models chosen to represent the responses for were very significant, meaning that the models are very useful for predicting the responses (Yi et al., 2009). Furthermore, the "lack of fit" p value for all the response models were greater than 0.05 indicating that the lack of fit was not significant. Significant lack of fit is not desirable as it implies that the model does not fit the experimental data (Myers et al., 2009).

Table 3: ANOVA results for model representing CH_4 recovered

Source	Sum of squares	Degree of freedom	Mean square	F value	p value
Model	2194.48	14	156.75	56.33	< 0.0001
X_1	1483.13	1	1483.13	532.99	< 0.0001
X_2	108.67	1	108.67	39.05	< 0.0001
X_3	283.92	1	283.92	102.03	< 0.0001
X_4	1.18	1	1.18	0.43	0.5248
X_1X_2	1.73	1	1.73	0.62	0.4432
X_1X_3	11.94	1	11.94	4.29	0.0573
X_1X_4	2.45	1	2.45	0.88	0.3636
X_2X_3	6.96	1	6.96	2.50	0.1361
X_2X_4	0.78	1	0.78	0.28	0.6050
X_3X_4	0.044	1	0.044	0.016	0.9014
X_1^2	226.22	1	226.22	81.29	< 0.0001
X_2^2	6.24	1	6.24	2.24	0.1564
X_3^2	45.69	1	45.69	16.42	0.0012
X_4^2	0.82	1	0.82	0.29	0.5965
Residual	38.96	14	2.78		
Lack of fit	38.67	10	3.87	54.64	0.0801
Pure error	0.28	4	0.071		
Cor total	2233.44	28			

Table 4: ANOVA results for model representing CO_2 captured

Source	Sum of squares	Degree of freedom	Mean square	F value	p value
Model	1021.38	14	72.96	2.91	0.0275
X_1	180.22	1	180.22	7.18	0.0179

Corresponding author: Ajieh, M. U. ✉ mike.ajieh@gmail.com ✉ Department of Chemical Engineering, Delta State University, Oleh Campus, Delta State, Nigeria. *© 2020. Faculty of Tech. Education, ATBU Bauchi. All rights reserved*

Source	Sum of squares	Degree of freedom	Mean square	F value	p value
X_2	11.13	1	11.13	0.44	0.5162
X_3	277.33	1	277.33	11.06	0.0050
X_4	0.048	1	0.048	1.91E-03	0.9658
X_1X_2	1.66	1	1.66	0.066	0.8007
X_1X_3	305.00	1	305.00	12.16	0.0036
X_1X_4	5.87E-06	1	5.87E-06	2.34E-07	0.9996
X_2X_3	18.04	1	18.04	0.72	0.4107
X_2X_4	0.012	1	0.012	4.59E-04	0.9832
X_3X_4	0.23	1	0.23	9.36E-03	0.9243
X_1^2	67.54	1	67.54	2.69	0.1231
X_2^2	6.49	1	6.49	0.26	0.6189
X_3^2	132.49	1	132.49	5.28	0.0375
X_4^2	5.04	1	5.04	0.20	0.6608
Residual	351.16	14	25.08		
Lack of fit	351.12	10	35.11	3149.34	0.1011
Pure error	0.045	4	0.011		
Cor total	1372.54	28			

The level of fit between the experimental data and the models were assessed using other statistical parameters such as coefficient of determination, coefficient of variation, standard deviation, adequate precision etc as shown in Table 5. As seen from the results presented in Table 5, all the models were characterised by high R^2 values indicating very good fit between the experimental observations and model predictions. Furthermore, the adjusted R^2 values obtained were within reasonable agreement with the corresponding R^2 values further confirming the fit of the models (Yi et al., 2009). The values of standard deviation were small compared to the mean of the observations showing that there was minimal dispersion of each individual observation about the mean (Myers et al., 2009). This further confirmed the significant fit of the models. The coefficient of variation (CV) is the standard deviation expressed as a percentage of the mean. It is a statistical parameter used to assess the reliability and repeatability of the experiments. Low CV values like those presented in Table 5 usually indicate that the experimental runs are reliable and repeatable. The adequate precision is a measure of the signal to noise ratio. Values greater than 4 are usually recommended. The values obtained as shown in Table 5 were all greater than 4 and this is an indication of adequate signal and the models can thus be used to navigate the design space (Myers et al., 2009).

Table 6: Goodness of fit statistics for RSM models

Response	R^2	Adjusted R^2	Mean	Standard deviation	CV %	Adeq. precision
CH_4 recovered	0.9826	0.9651	78.20	1.67	2.13	27.23
CO_2 captured	0.7442	0.6552	83.31	5.01	6.01	7.81

Corresponding author: Ajieh, M. U. ✉ mike.ajieh@gmail.com ✉ Department of Chemical Engineering, Delta State University, Oleh Campus, Delta State, Nigeria. *© 2020. Faculty of Tech. Education, ATBU Bauchi. All rights reserved*

Artificial Neural Network Modelling

The training algorithm for a neural network is unique to every process (Dorofki et al., 2012). Similarly, it is also not possible to determine apriori, the algorithm that will be most suitable for training a network. Thus, there was the need to iteratively investigate several training algorithms with the aim of determining the one that is most suitable for the process. The results presented in Table 7 shows that a multilayer full feed forward neural network trained with Levenberg-Marquardt learning algorithm was the best network architecture for predicting for the upgrading process. This was chosen because it had the highest R^2 value (0.9999 and 1.0000) and the lowest RMSE value (0.1014 and 0.0338) respectively for CH_4 recovery and CO_2 capture.

Table 7: ANN training algorithm for predicting CH_4 recovered and CO_2 captured

Network architecture	Training algorithm	CH_4 recovered		CO_2 captured	
		R^2	RMSE	R^2	RMSE
MNFF	IBP	0.9996	0.1866	0.9996	0.1437
	BBP	0.9981	0.3897	0.9998	0.0883
	QP	0.9963	0.5421	0.9991	0.2150
	GA	0.9947	0.6487	0.9965	0.4114
	LM	0.9999	0.1061	1.0000	0.0338
MFFF	IBP	0.9988	0.3152	0.9996	0.1478
	BBP	0.9995	0.1982	0.9999	0.0541
	QP	0.9801	1.251	0.9995	0.1557
	GA	0.9971	0.4776	0.9557	1.4729
	LM*	0.9999	0.1014	1.0000	0.0338

*Best learning algorithm and network

An iterative process was also used to determine the optimum number of neurons in the network. Different neural networks with different number of neurons were investigated and the results are shown in Table 8. As can be seen from the results obtained, the R^2 value increased as the number of neurons was increased from 1 to 4. The RMSE of both responses was observed to decrease as the number of neurons was increased from 1 to 4. This is an indication that the predictive capability of the network was increasing. However, increasing the number of neurons beyond 4 did not result in any change in the R^2 and RMSE values showing that the predictive capability of the network was not enhanced beyond 4 neurons. Thus, the optimum number of neurons for the network was chosen as 4. Hence, for a neural network with four input factors, 4 neurons in the hidden layer and 1 factor in the output layer, the corresponding optimum neural networks will be 4-4-1. The network architectures for both responses are represented schematically as shown in Figures 7 and 8 for both responses.

The predicted response levels of CH_4 recovery and CO_2 capture using the optimum neural network architecture and the actual experimental values are presented in Table 9 for comparison. It can be seen from the results presented that the values predicted by the ANN model were very close to the experimental values indicating validity and reliability of the ANN model.

Corresponding author: Ajieh, M. U. ✉ *mike.ajieh@gmail.com* ✉ *Department of Chemical Engineering, Delta State University, Oleh Campus, Delta State, Nigeria.* *© 2020. Faculty of Tech. Education, ATBU Bauchi. All rights reserved*

Table 8: Optimum number of neurons

No of neurons	CH_4 recovered		CO_2 captured	
	R^2	RMSE	R^2	RMSE
1	0.8973	2.8577	0.9293	1.8600
2	0.9909	0.8498	0.9983	0.2851
3	0.9978	0.4178	0.9988	0.2394
4*	0.9999	0.1014	1.0000	0.0338
5	0.9999	0.1014	1.0000	0.0338

* Optimum number of neurons

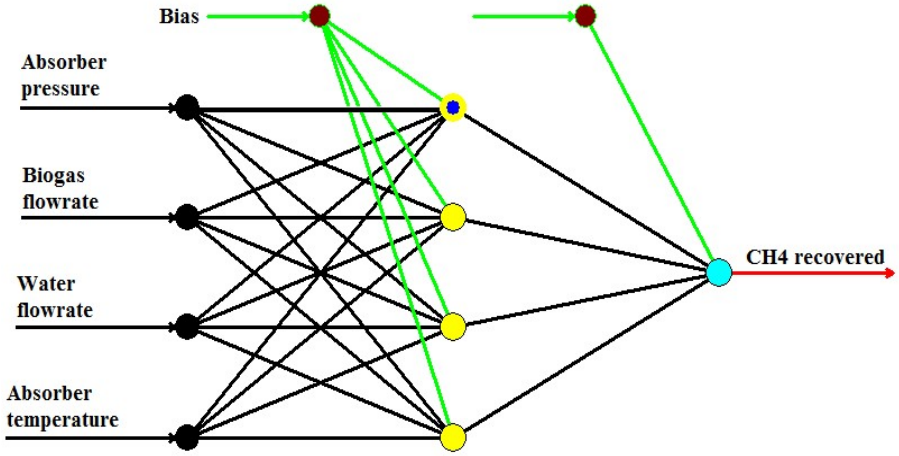

Figure 7: Optimal ANN architecture for predicting CH_4 recovered

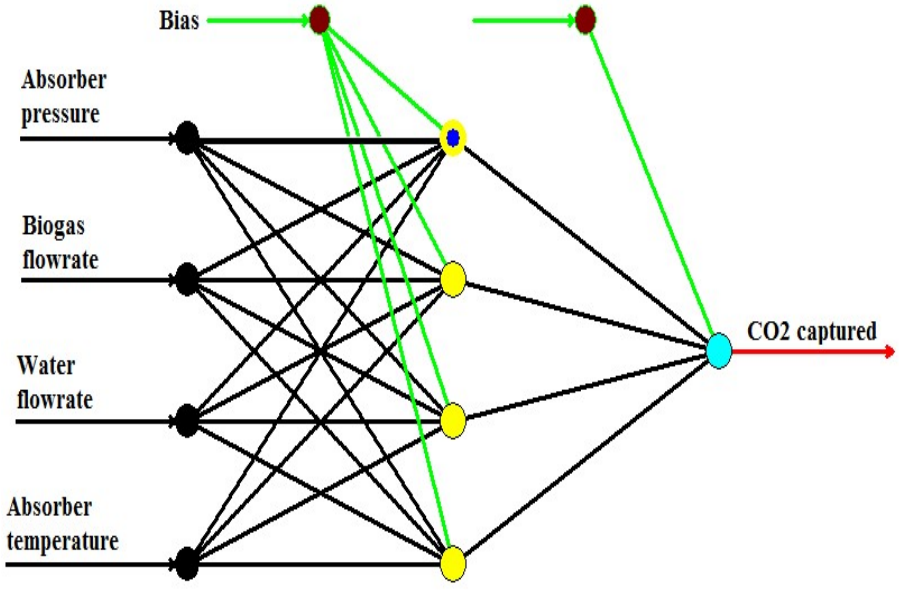

Figure 8: Optimal ANN architecture for predicting CO_2 captured

Corresponding author: Ajieh, M. U. ✉ mike.ajieh@gmail.com ✉ Department of Chemical Engineering, Delta State University, Oleh Campus, Delta State, Nigeria. *© 2020. Faculty of Tech. Education, ATBU Bauchi. All rights reserved*

JOURNAL OF SCIENCE TECHNOLOGY AND EDUCATION 8(3), SEPTEMBER, 2020
ISSN: 2277-0011; Journal homepage: www.atbuftejoste.com

Table 9: Comparison of experimental results with ANN predicted results

Run	Factors								Responses			
	Coded values				Actual values				CH_4 recovered (%)		CO_2 captured (%)	
	X_1	X_2	X_3	X_4	X_1	X_2	X_3	X_4	Exp.	RSM	Exp.	RSM
1	0	0	-1	-1	12.5	9.5	50	5.0	73.7	73.7	81.7	81.7
2	0	1	0	-1	12.5	12.0	125	5.0	77.5	77.5	85.4	85.4
3	1	-1	0	0	20.0	7.0	125	22.5	88.9	88.9	85.7	85.7
4	-1	0	1	0	5.0	9.5	200	22.5	64.7	64.7	84.9	84.9
5	-1	-1	0	0	5.0	7.0	125	22.5	65.2	65.2	85.4	85.4
6	0	-1	1	0	12.5	7.0	200	22.5	89.4	89.4	85.7	85.7
7	0	0	0	0	12.5	9.5	125	22.5	81.7	81.2	85.9	85.7
8	0	0	-1	1	12.5	9.5	50	40.0	73.4	73.4	80.8	80.8
9	1	0	0	-1	20.0	9.5	125	5.0	85.1	85.1	85.7	85.7
10	0	1	1	0	12.5	12.0	200	22.5	80.7	80.7	85.7	85.7
11	0	0	1	1	12.5	9.5	200	40.0	82.9	82.9	85.7	85.7
12	1	1	0	0	20.0	12.0	125	22.5	85.1	85.1	85.7	85.7
13	-1	1	0	0	5.0	12.0	125	22.5	64.0	64.0	82.8	82.8
14	0	0	0	0	12.5	9.5	125	22.5	81.1	81.2	85.7	85.7
15	0	0	0	0	12.5	9.5	125	22.5	81.1	81.2	85.7	85.7
16	1	0	-1	0	20.0	9.5	50	22.5	78.4	78.4	84.5	84.5
17	1	0	1	0	20.0	9.5	200	22.5	89.8	89.8	85.7	85.7
18	0	1	0	1	12.5	12.0	125	40.0	79.3	79.3	85.6	85.6
19	1	0	0	1	20.0	9.5	125	40.0	88.3	88.3	85.7	85.7
20	0	1	-1	0	12.5	12.0	50	22.5	71.9	71.9	75.8	75.8
21	-1	0	0	1	5.0	9.5	125	40.0	64.2	64.2	82.3	82.3
22	-1	0	0	-1	5.0	9.5	125	5.0	64.2	64.2	82.4	82.4
23	0	0	0	0	12.5	9.5	125	22.5	81.1	81.2	85.7	85.7
24	0	-1	-1	0	12.5	7.0	50	22.5	75.3	75.3	84.3	84.3
25	0	0	1	-1	12.5	9.5	200	5.0	83.7	83.7	85.7	85.7
26	0	0	0	0	12.5	9.5	125	22.5	81.1	81.2	85.7	85.7
27	0	-1	0	1	12.5	7.0	125	40.0	87.9	87.9	85.7	85.7
28	-1	0	-1	0	5.0	9.5	50	22.5	60.2	60.2	48.8	48.8
29	0	-1	0	-1	12.5	7.0	125	5.0	87.9	87.9	85.7	85.7

The goodness of fit statistics for the models representing CH_4 recovered and CO_2 captured for the three upgrading strategies are presented in Table 4.43. The results show that the ANN prediction was characterised by very high R^2 and adjusted R^2 (R^2 and adjusted R^2~1.0000). They were also characterised by very low RMSE and AAD values. This shows that there was almost a perfect fit between the ANN model predictions and the experimental values.

Corresponding author: Ajieh, M. U. ✉ *mike.ajieh@gmail.com* ✉ *Department of Chemical Engineering, Delta State University, Oleh Campus, Delta State, Nigeria.* *© 2020. Faculty of Tech. Education, ATBU Bauchi. All rights reserved*

Table 10: Goodness of fit statistics for ANN

Parameter	Response	
	CH_4 recovered	CO_2 captured
R^2	0.9999	1.0000
Adj. R^2	0.9998	1.0000
RMSE	0.1200	0.0400
AAD	0.0003	0.0009

Comparison of RSM and ANN Performance

A performance evaluation was carried out to determine which of RSM and ANN was better in terms of their accuracy in predicting the responses (CH_4 recovered and CO_2 captured). Models with more predictive capability are more accurate when used in predicting responses (Betiku et al., 2014). The predictive capability of RSM and ANN was assessed using R^2 value, adjusted R^2 value, root mean square error (RMSE) and absolute average deviation (AAD) as shown in Table 11. Very accurate models are characterised by high R^2 and adjusted R^2 values as well as low RMSE and AAD values (Velu et al., 2016). The results presented in Table 11 show that the ANN prediction was characterised by very high R^2 and adjusted R^2 (R^2 and adjusted R^2 ~ 1.0000). They were also characterised by very low RMSE and AAD values. This shows that there was almost a perfect fit between the ANN model predictions and the experimental values. Based on these observations, it is clearly evident that the ANN model performed better in predicting the responses compared to the RSM model.

Table 11: Comparison of RSM and ANN predictive performance

Parameters	RSM		ANN	
	CH_4 recovered	CO_2 captured	CH_4 recovered	CO_2 captured
R^2	0.9826	0.7442	0.9999	1.0000
Adj. R^2	0.9651	0.9521	0.9998	1.0000
RMSE	1.3937	4.2042	0.1200	0.0400
AAD	0.0172	0.0475	0.0003	0.0009

EFFECT OF INPUT FACTORS ON RESPONSES

The effect of the input variables (absorber pressure, biogas flowrate, liquid flowrate and absorber temperature) on the responses (CH_4 recovered and CO_2 captured) was evaluated by using response surface plots. These are three-dimensional (3D) plots, and they were produced by varying two variables within the experimental range, and keeping the remaining two variables constant at their centre point values. Figure 9 shows the effect of the interaction between absorber pressure and biogas flowrate on the amount of methane recovered for the high-pressure water scrubbing process. The trend observed show that high values of pressure favoured the water scrubbing process. This is seen in the fact that the amount of methane in the upgraded biogas increased as the pressure in the absorber was increased. This could be attributed to the removal of the impurities in the biogas, which is facilitated by the increase in their solubility at high pressures (Cozma et al., 2015). The amount of methane in the upgraded biogas was not significantly influenced by the biogas flowrate compared to absorber pressure.

Corresponding author: Ajieh, M. U. ✉ mike.ajieh@gmail.com ✉ Department of Chemical Engineering, Delta State University, Oleh Campus, Delta State, Nigeria. *© 2020. Faculty of Tech. Education, ATBU Bauchi. All rights reserved*

Nevertheless, there was an inverse relationship between methane recovery and the biogas flowrate. A combination of high absorber pressure and low biogas flowrate resulted in optimal methane recovery. Similar observations have been reported by previous researchers (Cozma et al., 2015; Sugiharto and Hidayat, 2015; Morero et al., 2017).

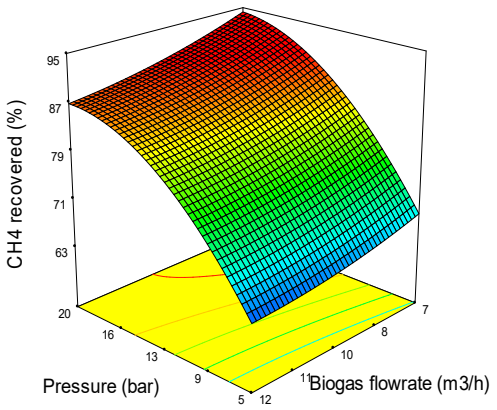

Figure 9: Response surface plot showing effect of absorber pressure and biogas flowrate on CH_4 recovered

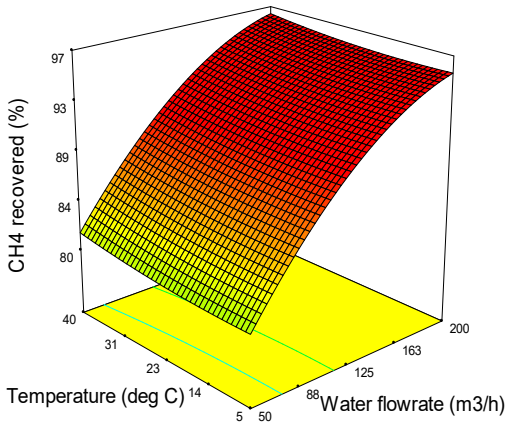

Figure 10: Response surface plot showing effect of temperature and water flow rate on CH_4 recovered

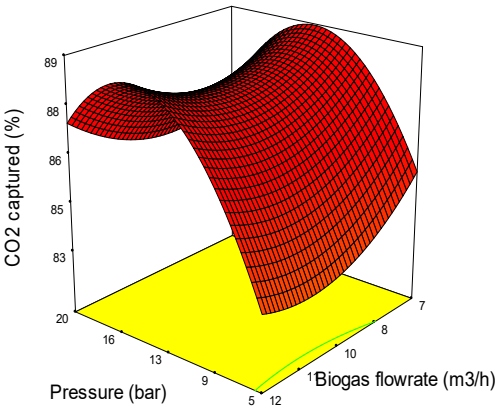

Figure 11: Response surface and contour plot showing effect of absorber pressure and biogas flowrate on CO_2 captured

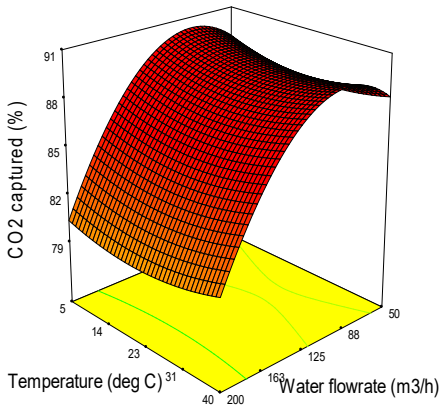

Figure 12: Response surface and contour plot showing effect of temperature and water flowrate on CO_2 captured

The effect of water flowrate and absorber temperature on methane recovery is shown in Figure 10. Increasing the water flowrate resulted in a significant increase in the amount of methane recovered in the upgrade biogas. This could be attributed to an increase in the mass transfer driving force, which facilitates the enhanced removal of the impurities from the raw biogas (Ndiritu et al., 2013). This observation is in line with the results of Aroonwilas et al. (2001) who attributed the increase in absorption efficiency to

Corresponding author: Ajieh, M. U. ✉ *mike.ajieh@gmail.com* ✉ *Department of Chemical Engineering, Delta State University, Oleh Campus, Delta State, Nigeria.* *© 2020. Faculty of Tech. Education, ATBU Bauchi. All rights reserved*

enhanced bulk absorption capacity of the liquid due to the increase in liquid molecules. Similar observations were also reported by previous researchers (Oi, 2007; Cozma et al., 2015; Sugiharto and Hidayat, 2015; Morero et al., 2017). Temperature did not have any significant effect on the absorption process as seen from Figure 10. This observation is corroborated by the fact that the p value for the model term representing temperature in the statistical model was greater than 0.05 indicating that it was not significant. Nevertheless, a combination of low temperature and high water flowrate resulted in optimum methane recovery.

The removal of CO_2 from the raw biogas as a function of absorber pressure and biogas flowrate is presented in Figure 11. The absorber pressure significantly enhanced the removal of CO_2 from the biogas stream as seen in the steep increase in CO_2 captured when the absorber pressure was increased. This observation can be directly linked to the fact that absorption of CO_2 by water is governed by Henry's law. Thus, the absorption process will be facilitated at high pressures (Cozma et al., 2013). The absorption of CO_2 was better at lower biogas flowrates. This could be as a result of the increase in the CO_2 loading as the biogas flowrate was increased. The increased CO_2 loading does not favour the process in terms of mass transfer characteristics because the mass transfer driving force would have been increased (Abdul Halim et al., 2015). The increase in the removal of CO_2 from the raw biogas as a function of absorber pressure and water flowrate is directly related to the increase in the recovery of methane in the upgraded biogas. Higher water flowrates was found to be favourable for the removal of CO_2 while temperature did not have any significant influence on the process as shown in Figure 12.

Optimisation of Input Factors and Responses

Numerical optimisation of the responses was carried out using the Design Expert software. The values of the independent variables were fixed within the experimental range while the responses were maximized. The results of the analysis are shown in Table 12. The high-pressure water scrubbing process recorded 93% methane in the upgraded biogas stream with a corresponding CO_2 removal level of 87%. These results were validated by carrying out triplicate experiments at the recorded optimum conditions. The mean values of the triplicate experiments were comparable to the prediction of the statistical models.

Table 12: Optimization results

Variable	Value
Absorber pressure	18 bar
Biogas flow rate	7 m^3/h
Water flow rate	148 m^3/h
Absorber temperature	11 ^oC
Maximum CH_4 recovered	93%
Maximum CO_2 captured	87%

CONCLUSION

The following conclusions can be drawn from the results of this work.

1. ANN is a better predictive tool compared to RSM
2. CH_4 recovery and CO_2 captured during biogas upgrading via HPWS can be represented by validated quadratic models

Corresponding author: Ajieh, M. U. ✉ mike.ajieh@gmail.com ✉ Department of Chemical Engineering, Delta State University, Oleh Campus, Delta State, Nigeria. *© 2020. Faculty of Tech. Education, ATBU Bauchi. All rights reserved*

3. CH_4 recovery is significantly influenced by absorber pressure, biogas flow rate, water flow rate but not temperature
4. CO_2 captured is significantly influenced by absorber pressure and water flow rate but not biogas flow rate and temperature

REFERENCES

Abdeen, F. R., Mel, M., Jami, M. S., Ihsan, S. I. and Ismail, A. F. (2016). A review of chemical absorption of carbon dioxide for biogas upgrading. *Chinese Journal of Chemical Engineering*, *24*(6), pp. 693-702.

Abdul Halim, H. N., M. Shariff, A., Tan, L. S. and Bustam, M. A. (2015). Mass transfer performance of CO2 absorption from natural gas using monoethanolamine (MEA) in high-pressure operations. *Industrial & Engineering Chemistry Research*, *54*(5), pp. 1675-1680.

Ajieh, U. M., Onochie., U. P, Kubeyinje. B. F, Orerome., R.T. and Akingba, O. (2016). Biogas Production from a Blend of Water Hyacinth - *Eichhornia crassipes* (Martius) Solmslaubach (Pontederiaceae) and Cattle Rumen Waste (Dung). *International Journal of Renewable. Energy & Environment,* 2, pp. 32-41.

Ajieh, M. U., Muhammed, J. I. and Ogbeide, S. E. (2018). Biomethane potential of selected faecal manure for digestion and co-digestion in biogas production. *Nigerian Research Journal of Engineering and Environmental Sciences*, 3(1), pp. 472-476.

Amenaghawon, N. A., Oiwoh, O. and Ebewele, O. E. (2015). Optimisation of fermentation conditions of citric acid production from banana peels using response surface methodology. *Nigerian Journal of Technology*, *34*(4), pp. 716-723.

Amenaghawon, N. A. and Amagbewan, E. (2017). Evaluating the effect of acid mixtures and solids loading on furfural production from sugarcane bagasse: optimization using response surface methodology and artificial neural network. *Nigerian Research Journal of Engineering and Environmental Sciences*, 2(2), pp. 578-587.

Aroonwilas, A., Tontiwachwuthikul, P. and Chakma, A. (2001). Effects of operating and design parameters on CO2 absorption in columns with structured packings. *Separation and Purification Technology*, *24*(3), pp. 403-411.

Asfaram, A., Ghaedi, M., Azqhandi, M. A., Goudarzi, A. and Dastkhoon, M. (2016). Statistical experimental design, least squares-support vector machine (LS-SVM) and artificial neural network (ANN) methods for modeling the facilitated adsorption of methylene blue dye. *RSC Advances*, *6*(46), pp. 40502-40516.

AspenTech (2017). A History of Innovation. www.aspentech.com- (Assessed March 22nd, 2018)

Awe, O. W., Zhao, Y., Nzihou, A., Minh, D. P. and Lyczko, N. (2017). A review of biogas utilisation, purification and upgrading technologies. *Waste and Biomass Valorization*, *8*(2), pp. 267-283.

Bas, D. and Boyaci, I. H. (2007). Modeling and optimization II: comparison of estimation capabilities of response surface methodology with artificial neural networks in a biochemical reaction. *Journal of Food Engineering*, *78*(3), pp. 846-854.

Corresponding author: Ajieh, M. U. ✉ mike.ajieh@gmail.com ✉ Department of Chemical Engineering, Delta State University, Oleh Campus, Delta State, Nigeria. *© 2020. Faculty of Tech. Education, ATBU Bauchi. All rights reserved*

Betiku, E., Okunsolawo, S. S., Ajala, S. O. and Olatunde, S.O. (2014). Performance evaluation of artificial neural network coupled with generic algorithm and response surface methodology in modeling and optimization of biodiesel production process parameters from shea tree (*Vitellaria paradoxa*) nut butter. *Renewable Energy,* 76, pp. 408-417.

Chapoy, A., Mohammadi, A. H., Richon, D. and Tohidi, B. (2004). Gas solubility measurement and modeling for methane–water and methane–ethane–n-butane–water systems at low temperature conditions. *Fluid Phase Equilibria*, *220*(1), pp. 111-119.

Cozma, P., Wukovits, W., Mămăligă, I., Friedl, A. and Gavrilescu, M. (2013). Analysis and modelling of the solubility of biogas components in water for physical absorption processes. *Environmental Engineering & Management Journal (EEMJ)*, *12*(1), pp. 147-162.

Cozma, P., Wukovits, W., Mămăligă, I., Friedl, A. and Gavrilescu, M. (2015). Modeling and simulation of high pressure water scrubbing technology applied for biogas upgrading. *Clean Technologies and Environmental Policy*, *17*(2), pp. 373-391.

Foroughi, M., Rahmani, A. R., Asgari, G., Nematollahi, D., Yetilmezsoy, K. and Samarghandi, M. R. (2018). Optimization of a three-dimensional electrochemical system for tetracycline degradation using box-behnken design. *Fresenius Environmental Bulletin*, *27*(3), pp. 1914-1922.

International Energy Agency (IEA) (2000). Bioenergy. Biogas upgrading and utilisation. In: Wheeler, P., Jaatinen, T., Lindberg, A., Lundeberg, S., Holm-Nielsen, J.B., Wellinger, A. (Eds). Task 24: Energy from biological conversion of organic waste. Paris, France. Available at: http://www.biores.eu/docs/BIOGASFUNDAMENTALS/Biogas_upgrading__utili sation.pdf

Kapoor, R., Subbarao, P. M. V., Vijay, V. K., Shah, G., Sahota, S., Singh, D. and Verma, M. (2017). Factors affecting methane loss from a water scrubbing based biogas upgrading system. *Applied Energy*, *208*, pp. 1379-1388.

Khan, I. U., Othman, M. H. D., Hashin, H., Matsumara, T., Ismail, A. F., Rezaei-DashtArzhandi, M. Azalee, I.W. (2017). Biogas as a renewable energy fuel – A review of biogas upgrading, utilisation and storage. *Energy Conversion Management*, 150, pp. 277-294.

Lucas, E. B. and Bamgboye, A. I. (1998). Anaerobic digestion of chopped water hyacinth. *Nigerian Journal of Renewable Energy*, 6 (1), pp. 62-66.

Malinauskaite, J., Jouhara, H., Czajczyńska, D., Stanchev, P., Katsou, E., Rostkowski, P. and Anguilano, L. (2017). Municipal solid waste management and waste-to-energy in the context of a circular economy and energy recycling in Europe. *Energy*, *141*, pp. 2013-2044.

Maria, G. (2008). Biomass Power for Energy and Sustainable Development. *Environmental Engineering and Management Journal, Romania*, 7(5), pp. 617-640.

Morero, B., Groppelli, E. S. and Campanella, E. A. (2017). Evaluation of biogas upgrading technologies using a response surface methodology for process simulation. *Journal of cleaner production*, *141*, pp. 978-988.

Corresponding author: Ajieh, M. U. ✉ mike.ajieh@gmail.com ✉ Department of Chemical Engineering, Delta State University, Oleh Campus, Delta State, Nigeria. *© 2020. Faculty of Tech. Education, ATBU Bauchi. All rights reserved*

Myers, R. H., Montgomery, D. C. and Anderson-Cook, C. M. (2009). *Response Surface Methodology: Process and Product Optimization Using Designed Experiments*. Wiley Series in Probability and Statistics.

Ndiritu, H., Kibicho, K. and Gathitu, B. B. (2013). Influence of flow parameters on capture of carbon dioxide gas by a wet scrubber. *Journal of Power Technologies*, *93*(1), pp. 9-15.

Oi, L.E. (2007). Aspen HYSYS simulation of CO_2 removal by amine absorption from a gas-based power plant. In *The 48th Scandinavian Conference on Simulation and Modeling (SIMS 2007); 30-31 October; 2007; Göteborg (Särö)* (No. 027, pp. 73-81). Linköping University Electronic Press.

Petersson, A. and Wellinger, A. (2009). Biogas upgrading technologies—developments and innovations. *IEA Bioenergy*, 37, pp. 1–15.

Sugiharto, A. and Hidayat, M. (2015). Sensitivity analysis of water scrubbing process for biogas Purification. *ICETEA Proceedings*. pp. 35-39

Sun, Q., Hailong, L., Jinying, Y., Longcheng, L., Zhixin, Y. and Xinhai, Y. (2015). Selection of appropriate biogas upgrading technology-a review of biogas cleaning, upgrading and utilisation. *Renewable and Sustainable Energy Reviews*, 51, pp. 521-532.

Valtz, A., Chapoy, A., Coquelet, C., Paricaud, P. and Richon, D. (2004). Vapour–liquid equilibria in the carbon dioxide–water system, measurement and modelling from 278.2 to 318.2 K. *Fluid phase equilibria*, *226*, pp. 333-344.

Velu, S., Velayutham, V. and Manickkam, S. (2016). Optimization of fermentation media for xanthan gum production from Xanthomonas campestris using Response Surface Methodology and Artificial Neural Network techniques. *Indian Journal of Chemical Technology,* 23, pp. 353-361.

Yi, S., Su, Y., Qi, B., Su, Z. and Wan, Y. (2009). Application of response surface methodology and central composite rotatable design in optimizing the preparation conditions of vinyltriethoxysilane modified silicalite/polydimethylsiloxane hybrid pervaporation membranes. *Separation and Purification Technology*, 71(2), pp. 252-262.

Zhang, J., Loh, K. C., Lee, J., Wang, C. H., Dai, Y. and Tong, Y. W. (2017). Three-stage anaerobic co-digestion of food waste and horse manure. *Scientific reports*, *7*(1), pp. 1-10.

Corresponding author: Ajieh, M. U. ✉ mike.ajieh@gmail.com ✉ Department of Chemical Engineering, Delta State University, Oleh Campus, Delta State, Nigeria. *© 2020. Faculty of Tech. Education, ATBU Bauchi. All rights reserved*